

## ORIGINAL RESEARCH—CLINICAL

## Discovery and Validation of Methylated DNA Markers From Pancreatic Neuroendocrine Tumors



Shounak Majumder,<sup>1</sup> Thorvardur R. Halfdanarson,<sup>2</sup> Calise K. Berger,<sup>1</sup> Patrick H. Foote,<sup>1</sup> Xiaoming Cao,<sup>1</sup> Maria C. McGlinch,<sup>1</sup> Brianna J. Gysbers,<sup>1</sup> Jaime de La Fuente,<sup>1</sup> Mariah J. Robran,<sup>1</sup> Karen A. Doering,<sup>1</sup> Kelli N. Burger,<sup>3</sup> William E. Bamlet,<sup>3</sup> Ann L. Oberg,<sup>4</sup> Douglas W. Mahoney,<sup>3</sup> Rondell P. Graham,<sup>5</sup> William R. Taylor,<sup>4</sup> Gloria M. Petersen,<sup>6</sup> and John B. Kisiel<sup>1</sup>

<sup>1</sup>Division of Gastroenterology and Hepatology, Mayo Clinic, Rochester, Minnesota; <sup>2</sup>Division of Medical Oncology, Mayo Clinic, Rochester, Minnesota; <sup>3</sup>Division of Clinical Trials and Biostatistics, Mayo Clinic, Rochester, Minnesota; <sup>4</sup>Division of Quantitative Health Sciences, Mayo Clinic, Rochester, Minnesota; <sup>5</sup>Division of Anatomic Pathology, Mayo Clinic, Rochester, Minnesota; and <sup>6</sup>Division of Epidemiology, Mayo Clinic, Rochester, Minnesota

**BACKGROUND AND AIMS:** Methylated DNA markers (MDMs) accurately identify several different cancer types, but there are limited data for pancreatic neuroendocrine tumors (pNETs). We aimed to identify MDM candidates in tissue that differentiate pNETs from normal pancreas. **METHODS:** We used DNA from frozen normal pancreas (13) and pNET (51) tissues, we performed reduced representation bisulfite sequencing for MDM discovery. Validation in independent formalin fixed paraffin embedded tissues used pNET cases (67; solid = 50, cystic = 17), normal pancreas (24), and buffy coat (36) controls. Primary pNET MDM distributions were compared with lung (36), small bowel (36) NETs, and metastatic pNET (25) tissues. The discrimination accuracy was summarized as the area under the receiver operator characteristic curve (AUC) with corresponding 95% confidence intervals (CIs). Fisher's linear discriminant analysis was performed to estimate a linear discriminate score (LDS) differentiating normal from pNET tissue and applied to all patient groups; discrimination accuracy of the LDS was summarized as the bootstrap cross-validated AUC. **RESULTS:** Median AUC for distinguishing normal pancreas from pNET tissue was 0.91 (interquartile range: 0.80–0.93). The cross-validated AUC for the LDS discriminating normal pancreatic tissue from primary and metastatic pNETs was 0.957 (95% CI 0.858–1.0,  $P < .0001$ ) and 0.963 (95% CI 0.865–1.0,  $P < .0001$ ), respectively. The LDS for the MDM panel was significantly higher for primary pNET, metastatic pNET, lung NET, and small bowel NET, each compared with normal pancreas tissue ( $P < .0001$ ). There was no statistical difference between primary pNET and metastatic pNET ( $P = .1947$ ). **CONCLUSION:** In independent tissue validation, MDMs accurately discriminate pNETs from normal pancreas. These results provide scientific rationale for exploration of these tissue MDMs in a plasma-based assay for clinical application.

**Keywords:** Neuroendocrine Tumors; DNA Methylation; Biomarker; Pancreatic Neoplasms

tumors and can present as a solid or cystic pancreatic lesion. The prevalence of pNETs in the United States has increased in the last decade, largely due to incidental detection with widespread diagnostic use of high-definition abdominal imaging.<sup>1,2</sup> The vast majority of pNETs are nonfunctioning and do not present with a clinical syndrome of hormone overproduction. Despite being clinically silent, pNETs can be biologically aggressive and may manifest with metastatic disease at the time of initial detection, irrespective of size of the primary lesion. Currently, the World Health Organization (WHO) classifies all NETs into low grade (G1), intermediate grade (G2), and high grade (G3) categories based upon mitotic count and/or proliferative index (Ki-67) assessed in pancreatic tumor tissue. There is a paucity of reliable noninvasive biomarkers for accurately detecting pNETs. Both diagnosis and assessment of biological behavior are largely dependent on tissue sampling and are challenging for small lesions due to poor diagnostic tissue yield and associated risk of pancreatitis. In patients who undergo pancreatic resection, recurrence is not uncommon and can occur several years after surgery, warranting long-term surveillance.<sup>3–5</sup> For patients with a metastatic disease, current pharmacotherapies can achieve an objective response but rarely eradicate the tumor. Biomarkers for reliably monitoring disease activity during treatment would be clinically impactful. Thus, there is a need for identifying novel pNET biomarkers that can be applied to diagnosis, staging,

**Abbreviations used in this paper:** AUC, area under the receiver operator characteristic curve; CI, confidence interval; DMR, differentially methylated region; IRB, Institutional Review Board; LDS, linear discriminate score; MDM, methylated DNA marker; PDAC, pancreatic ductal adenocarcinoma; pNET, pancreatic neuroendocrine tumor; qMSP, quantitative methylation-specific PCR; RRBS, reduced representation bisulfite sequencing; WHO, World Health Organization.

Most current article

Copyright © 2022 The Authors. Published by Elsevier Inc. on behalf of the AGA Institute. This is an open access article under the CC BY-NC-ND license (<http://creativecommons.org/licenses/by-nc-nd/4.0/>).

2772-5723

<https://doi.org/10.1016/j.gastha.2022.01.006>

## Introduction

Pancreatic neuroendocrine tumors (pNETs) account for a small but important subset of pancreatic

and surveillance. We have previously published DNA methylation marker discovery by next-generation sequencing and validation of novel methylated DNA markers (MDMs) for detecting pancreatic ductal adenocarcinoma (PDAC) in tissue that has subsequently led to identification of MDM panels in pancreatic cyst fluid, pancreatic juice, and peripheral blood that accurately discriminate PDAC from healthy controls.<sup>6–8</sup> Recent reports also indicate a role of DNA methylation in pNET tumorigenesis and a potential link between methylation, histologic grade, and clinical prognosis.<sup>9,10</sup> We hypothesized that an unbiased methylome discovery and validation effort in tissue from pNETs will identify candidate MDMs that distinguish pNETs from normal pancreas tissue and buffy coat. If borne out, these MDMs can be subsequently explored in plasma for diagnosis, monitoring disease progression, and postoperative surveillance. Furthermore, MDMs that are expressed in pNETs but not in normal pancreas or other primary NETs may be ideally suited in the future for diagnosis, and those that are expressed in both primary and metastatic tissues from the same patient would be ideally suited for disease surveillance after systemic therapy or surgical resection of the primary tumor. In this study, our primary aim was to identify and validate discriminant tissue MDM candidates that differentiate cases with pNET, including both solid and cystic phenotypes, from normal pancreas tissue and buffy coat controls. Secondly, we aimed to compare the tissue DNA methylation profile of primary pNETs with primary extrapancreatic NETs and with metastatic pNET deposits using paired primary and metastatic tissue samples.

## Methods

### Study Overview and Patient Samples

All study procedures were approved by the Mayo Clinic Institutional Review Board (IRB). The Mayo Clinic IRB follows the requirements of the U.S. Food and Drug Administration (FDA) regulations 21 CFR Parts 50 and 56 and the U.S. Department of Health and Human Services regulations 45 CFR 46, which are guided by the Belmont Report. The Mayo Clinic IRB complies with the International Council for Harmonization of Technical Requirements for Pharmaceuticals for Human Use Guidelines on Good Clinical Practices, consistent with FDA and Health and Human Services regulations. The frozen case tissue samples of both pNET and normal pancreatic tissue were obtained from the Mayo Clinic Pancreas Cancer SPORE Registry (P50 CA102701), sequentially recruited patients with pancreatic neoplasms for enrollment since September 2000. For discovery of MDMs by reduced representation bisulfite sequencing (RRBS), frozen pancreatic tissues were obtained from pNET cases including both solid and cystic tumors, and control samples consisted of normal pancreatic tissue and normal buffy coat. Normal control pancreatic tissue was obtained from surgical resection specimens of benign pancreatic disease including chronic pancreatitis and serous cystadenoma but not from the field of resected pNETs or other pancreatic malignancies. Normal buffy coat from healthy controls was included to minimize leukocyte background methylation for future application of MDMs in noninvasive blood-based testing. The normal buffy coat samples were obtained from a biorepository for healthy controls enrolled from a

7-county regional population; those with a cancer diagnosis <5 years prior to enrollment or <3 years after enrollment were excluded. Area under the receiver operator characteristic curve (AUC), fold-change, and *P*-value criteria were used to select candidates' MDMs from the sequencing experiment for blinded validation in independent formalin fixed paraffin embedded (FFPE) tissue. For biological validation, paraffin-embedded tissues from independent case and control groups were obtained from the Mayo Clinic Tissue Registry and assayed by quantitative methylation-specific PCR (qMSP). Case tissues for validation included primary pNET, lung NET, small bowel NET, and metastatic pNET. These tissues were obtained from the Mayo Clinic Pancreas Cancer SPORE Registry as well as the Center for Cell Signaling Clinical Core (P30DK084567). Tissue samples from patients with a prior history of PDAC, those who received chemotherapy class drugs in the past 6 months, or those who had therapeutic radiation to the abdomen were excluded from the study. Tissues were macrodissected and histology reviewed by an expert pathologist (R.P.G). Samples were age- and sex-balanced, randomized, and blinded. DNA from tissues and blood samples were purified using the Qiagen QIAamp FFPE tissue kit and QIAamp DNA Blood Mini kit (Qiagen, Valencia, CA), respectively. DNA was repurified with AMPure XP beads (Beckman-Coulter, Brea, CA) and quantified by PicoGreen fluorescence (Thermo-Fisher, Waltham, MA). DNA integrity was assessed using qPCR.

### Assay Techniques

**Discovery.** RRBS sequencing libraries were prepared using the NuGEN Ovation RRBS Methyl-Seq kit with modifications (Tecan Genomics, Redwood City, CA). Samples were combined in a 4-plex format and sequenced by the Mayo Genomic Analysis Core facility on the Illumina HiSeq 4000 instrument (Illumina, San Diego, CA). Reads were processed by Illumina pipeline modules for image analysis and base calling. Secondary analysis was performed using SAAP-RRBS, a Mayo-developed bioinformatics suite.<sup>11</sup> Briefly, reads were cleaned up using Trim Galore and aligned to the GRCh37/hg19 reference genome build with Bisulfite sequence MAPPING program. Methylation ratios were determined by calculating  $C/(C + T)$ , or conversely  $G/(G + A)$  for reads mapping to reverse strand, for CpGs with coverage  $\geq 10X$  and base quality score  $\geq 20$ . Individual CpGs were ranked by hypermethylation ratio, namely the number of methylated cytosines at a given locus over the total cytosine count at that site. CpG hypermethylation was defined as least 20% methylation in cases compared with  $\leq 5\%$  in tissue controls or  $\leq 1\%$  for buffy coat controls. CpGs that did not meet these criteria were discarded. Subsequently, candidate CpGs were binned by genomic location into differentially methylated regions (DMRs) ranging from approximately 40 to 220 bp with a minimum cutoff of 5 CpGs per region. DMRs with an excessively high CpG density ( $>30\%$ ) were excluded to avoid GC-related amplification problems in the validation phase. Two analyses were performed comparing pNET tissue vs normal tissue controls and pNET tissue vs buffy coat controls. Following logistic regression, the 2 sets of DMRs were ranked by *P* value, AUC, and fractional methylation ratio between cases and all controls. No adjustments for false discovery were made during this phase, as independent validation was planned a priori.

**Marker Selection.** Using prespecified criteria, a subset of the DMRs was chosen for further development. The criteria were based on cutoffs of AUC ( $\geq 0.90$ ), methylation ratio ( $\geq 5$ ),

and  $P$  value ( $\leq 0.01$ ), for comparison between pNET and normal tissue; 72 DMRs met these criteria. For comparison of pNET tissue and buffy coat control samples, the cutoffs were 0.95, 100, and 0.01, respectively, resulting in 126 DMRs. These pools were further reduced by eliminating redundant DMRs (those which exhibited similar positivity across samples). DMRs that demonstrated robust sample-to-sample coordinated methylation (all or none at the CpG level) were given preference; downstream targeted amplification assays perform best with coordinated regional hypermethylation and hypomethylation. These subsequent filtering metrics further reduced the candidate pool 6-fold.<sup>12</sup>

**Validation.** qMSP Primers were designed for candidate regions using MethPrimer and QC checked on 20 ng (6250 equivalents) of positive and negative genomic methylation controls.<sup>6</sup> Multiple annealing temperatures were tested for optimal discrimination. Briefly, we aimed to identify CpG patterns that would be most amenable to targeted amplification assays, a low-cost but highly sensitive platform. Coordinated methylation across a DMR was the most desirable signature in cases, and oligonucleotides were designed to overlay multiple CpGs ensuring the strongest post-bisulfite hybridization binding and subsequent amplification. Controls were devoid of methylation at these sites. Fully methylated and unmethylated synthetic standards were used as quality checks to ensure the MDM assays were functioning properly. Validation was performed in 2 stages of qMSP. The first technical validation step consisted of retesting the sequenced DNA samples from the discovery experiment. This was done to verify that the DMRs were truly discriminant and to ensure that sequencing performance can be replicated using a targeted amplification method that relies on gene-specific primers instead of universal adaptors. The second biological validation step utilized a larger set of independent tissue samples including primary pNETs and metastatic pNETs, primary lung and small bowel NETs, normal pancreatic control tissues, and normal buffy coat samples. The primary comparison for biological validation was comparing the methylation profile of primary pNETs with normal control pancreatic tissue and normal buffy coat methylation. As a secondary aim to compare the methylation profile of metastatic pNETs to primary pNET tissue, we targeted metastatic deposits from individuals on whom we had paired tissue from the primary pNET site. In addition, tissue from primary nonpancreatic NETs were included in the validation stage to assess overlap of highly discriminate pNET MDMs with primary NETs at other common primary sites such as lung and small bowel. Tissues were identified and verified using expert clinical and pathological reviews. DNA purification was performed using the Qiagen QIAmp FFPE tissue kit. The EZ-96 DNA Methylation kit (Zymo Research, Irvine, CA) was used for the bisulfite conversion step. Ten nanograms of converted DNA (per marker) was amplified using SYBR Green detection on Roche 480 LightCyclers (Roche, Basel, Switzerland). Serially diluted universal methylated genomic DNA (Zymo Research) was used as a quantitation standard. A CpG agnostic ACTB ( $\beta$ -actin) assay was used as an input reference and normalization control. Results were expressed as methylated copies (specific marker)/copies of ACTB.

### Sample Size Estimate and Statistical Analysis Plan

**Discovery and Technical Validation.** The primary analysis used logistic regression models where the

endpoint was the total number of methylated reads relative to the total depth of coverage for the defined DMR. To account for overdispersion of the data, a quasi-likelihood function was used to estimate an inflation factor to adjust the standard error of the model. Varying the inflation factor of the binomial variance, the discovery phase was powered to detect a minimum odds ratio of 3 with 80% power assuming a 2-sided significance level of 5%. Assuming a minimum depth of coverage of 20 reads per CpG within a DMR, a minimum of 18 samples per group was deemed adequate for the discovery phase. The primary analysis used during technical validation was estimation of the AUC using the methods of DeLong et al<sup>13</sup> with corresponding 95% confidence intervals (CIs) for each individual marker. As this was a technical validation, the samples that were used were the same as the discovery phase, and no formal statistical sample size assessment was performed. Only markers that met or exceeded the DMR selection criteria (mentioned previously) were carried forward to the biological validation phase.

**Biological Validation.** Patient data were summarized as a median with corresponding 25th and 75th percentiles for continuous variables and percent of group totals for categorical variables. For biological validation, the primary endpoint was primary pNET compared with normal pancreas. Patients with strand counts of ACTB  $< 25$  were considered to have insufficient DNA content and not included in the analysis. To assess the discriminant ability of the entire panel of tissue-derived MDMs, Fisher's linear discriminant analysis was performed comparing primary pNETs to normal pancreas to estimate a linear discriminant score (LDS).<sup>14</sup> Estimated scoring was used to calculate the LDS for all patients and was summarized across patient groups using boxplots with comparisons based on the Wilcoxon Rank Sum test. To account for patients who have both primary and metastatic pNETs, a linear mixed effects model was used to calculate the statistical significance between these 2 subgroups. The discriminant accuracy of individual MDMs and for the panel of MDMs, LDS score was summarized as an AUC with corresponding 95% CI. For the LDS scoring, bootstrap cross-validation was used to summarize the out-of-bag AUC with corresponding 95% confidence limits.<sup>13</sup> Briefly, a random sample with replacement was taken from the original data set to create a training set of the same size as the original data set. Samples not selected for training were held out ("out-of-bag") for testing. The LDS was refit within the training set and applied to the test set. This whole process was repeated 500 times, and the median across the 500 iterations provided a cross-validated estimate of AUC with confidence limits based on the 2.5th and 97.5th percentiles. The receiving operating characteristic curve is depicted using locally weighted scatterplot smoothing of sensitivity as a function of 1-specificity. The statistical correlation of the LDS between paired primary pNET and metastatic pNET tissues was assessed using Spearman's correlation coefficient after standardizing both groups to the mean and standard deviation of normal controls. The minimum number of 36 cases per disease group was determined based on the desire that the half width of the 95% CI for sensitivity (at a prespecified specificity of 95%) would be no larger than  $\pm 10\%$  for individual MDMs or the LDS assuming an estimated sensitivity of 90%. For the number of controls, the desire was to have 80% power to detect an AUC of 0.85 or higher relative to a null AUC of 0.7 assuming a one-sided test of significance of 0.05. This required a minimum group size of 31. For AUCs of 0.9 or higher relative to 0.7, 16 patients per subgroup were required to have 80% power with a one-sided significance level of 0.05.

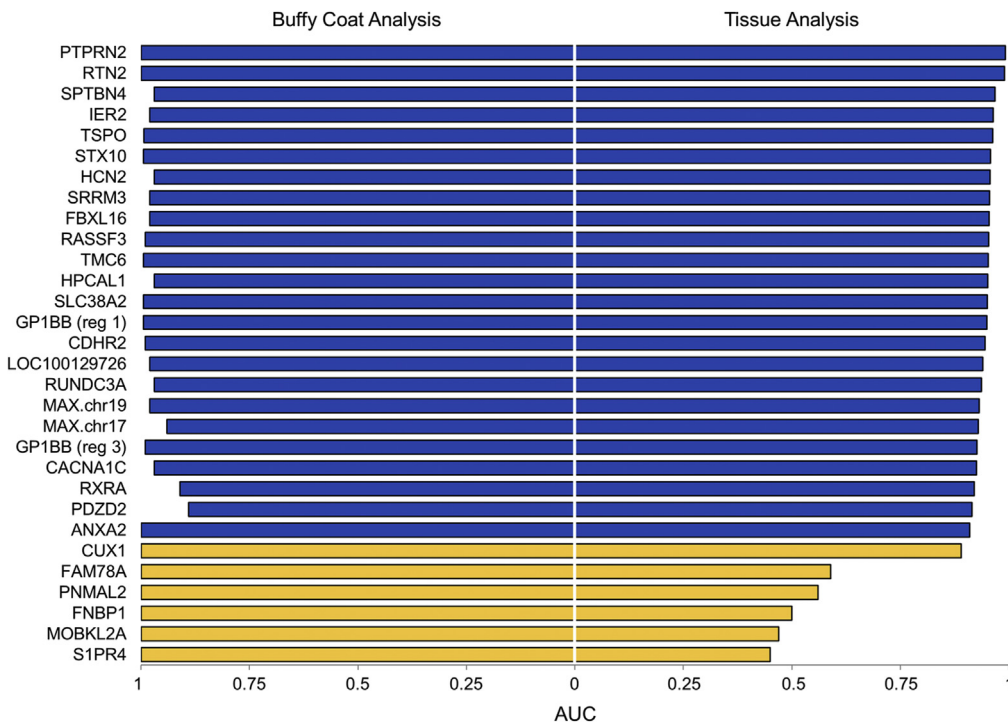


**Figure 1.** AUCs in tissue and buffy coat analysis in the discovery phase for the MDMs that met marker selection criteria for inclusion in biological validation.

## Results

### Discovery

RRBS was performed on DNA extracted from ethylenediamine tetraacetic acid (EDTA) normal buffy coat samples ( $n = 18$ ), frozen normal pancreas tissue ( $n = 13$ ), and pNET ( $n = 44$ ) tissue. The pNET cases included both solid ( $n = 28$ ) and cystic pNETs ( $n = 16$ ). Read counts for samples had at least 10X coverage for 4–5 million CpGs. Post-analysis and filtering (described previously) resulted in 198 hypermethylated pNET DMRs. Individual AUCs for regions that met selection criteria ranged from 0.90 to 1.00 with many exceeding 0.95. The pNET tissue and buffy coat comparison yielded the most dramatic differences in methylation signal, due to the specific epigenetic nature and signature of the 2 cell types. In contrast, the tissue analysis comparing normal pancreas and pNET tissue was less so. However, there were several MDMs (Figure 1) that exhibited high discrimination in both groups and were therefore selected for subsequent validation.

### Technical and Biological Validation

Thirty-three candidate DMRs that met selection criteria were chosen from the discovery set for further testing. Upon the *technical validation* of the discovery samples, 2 MDMs (*MYO15B* and *LGALS3*) showed lower discrimination ( $AUC < 0.90$ ) against the buffy coat samples than others and were not considered further. The remaining MDMs performed on par with the sequencing results and thus were taken forward into a blinded *biological validation* in independent FFPE tissues from primary pNET ( $n = 67$ ; solid = 50,

cystic = 17), normal pancreas controls ( $n = 24$ ), and normal buffy coat ( $n = 36$ ) using methylation-specific PCR. *CUX1* had a large DMR ( $>300$  bp) with varying degrees of coordinated methylation throughout, and 2 assays were designed for nonoverlapping CpGs, labeled *CUX1.v1* and *CUX1.v2*. MDM distributions in primary pNETs were compared with those in primary lung ( $n = 36$ ) and small bowel ( $n = 36$ ) NETs and metastatic pNET tissue ( $n = 25$ ). Eight patients had tissue samples with a strand count of *ACTB*  $<25$  and were not included in the analysis; this included 4 normal pancreas, 1 primary pNET, 1 metastatic pNET, 1 lung NET, and 1 small bowel NET. The clinical characteristics of all subjects included in the *biological validation* are listed in Table 1. Of the 23 metastatic pNETs with paired primary tissue, the primary pNET was solid in 21 and cystic in 2. Median Ki-67 in primary cystic pNETs was lower than that in solid pNETs and higher in metastatic tissue than that in the primary tumor (Table 1). The individual AUCs for MDMs in independent biological validation for discrimination of normal pancreas tissue from primary pNET tissue ranged from 0.33 to 0.96 (Table A1). At a high specificity cutoff of 95%, several MDMs discriminated NETs from normal pancreas irrespective of the primary site while some MDMs such as *PDZD2* and *CACNA1C* appeared to be more pancreas-specific (Figure 2). The linear discriminant score for the MDM panel was significantly higher for primary pNET, metastatic pNET, lung NET, and small bowel NET than that for normal pancreas tissue (all  $P < .0001$ ). There was no statistical difference between the primary pNET and metastatic pNET ( $P = .1947$ ). Compared with the primary pNET, there was a statistical difference for lung NET ( $P < .0001$ ) but not for small bowel NET ( $P = .3024$ ) (Figure 3A). The

**Table 1.** Clinical Characteristics of All Case and Control Tissue Samples in the Biological Validation Cohort

	Solid pNET (N = 49)	Cystic pNET (N = 17)	Metastatic pNET (N = 24)	Lung NET (N = 35)	Small bowel NET (N = 35)	Normal pancreas (N = 20)
<b>Age</b>						
Median (Q1, Q3)	55.4 (46.9, 63.9)	62.8 (50.9, 68.6)	55.3 (45.4, 61.6)	62.4 (50.7, 70.4)	60.3 (53.2, 66.7)	59.6 (37.5, 68.5)
<b>Sex</b>						
Male	28 (57.1%)	11 (64.7%)	16 (66.7%)	16 (45.7%)	21 (60.0%)	4 (20.0%)
<b>Race</b>						
Caucasian	43 (87.8%)	17 (100.0%)	19 (79.2%)	31 (88.6%)	32 (91.4%)	16 (80.0%)
<b>Tobacco use</b>						
Current	7 (14.9%)	3 (17.6%)	5 (21.7%)	4 (11.8%)	2 (5.9%)	2 (11.8%)
Former	13 (27.7%)	6 (35.3%)	6 (26.1%)	12 (35.3%)	12 (35.3%)	4 (23.5%)
Never	27 (57.4%)	8 (47.1%)	12 (52.2%)	18 (52.9%)	20 (58.8%)	11 (64.7%)
<b>Primary NET size (cm)</b>						
Median (Q1, Q3)	3.8 (2.5, 5.7)	2.9 (2.3, 3.6)	4.2 <sup>a</sup> (2.9, 6.8)	2.0 (1.4, 2.7)	1.7 (1.5, 2.1)	-
<b>Ki-67 (%)</b>						
Median (Q1, Q3)	7.0 (3.0, 12.0)	3.0 (2.0, 5.0)	12.5 <sup>a</sup> (7.8, 23.5)	3.0 (2.0, 7.0)	2.0 (1.0, 4.0)	-

<sup>a</sup>Twenty-three of 24 paired with primary pNET (2 cystic and 21 solid).

combined panel of MDMs demonstrated high discrimination in tissue-extracted DNA for both primary and metastatic pNETs with AUCs of 0.957 (95% CI 0.858–1) and 0.962 (95% CI 0.865–1), respectively (Figure 3B and C).

### Discussion

Aberrant DNA methylation is linked to carcinogenesis and broadly informative as a diagnostic biomarker in

multiple cancers.<sup>15–18</sup> However, there is currently no methylation-based biomarker available for detection of NETs, and the tissue methylation profile of pNETs across a spectrum of primary and metastatic sites has not been studied in detail. In this study, we describe tissue discovery and validation of a panel of MDMs that accurately distinguish pNETs from normal pancreatic tissue and buffy coat. Using paired primary pNET and metastatic pNET tissue, we demonstrate that tissue MDMs overlap for primary and

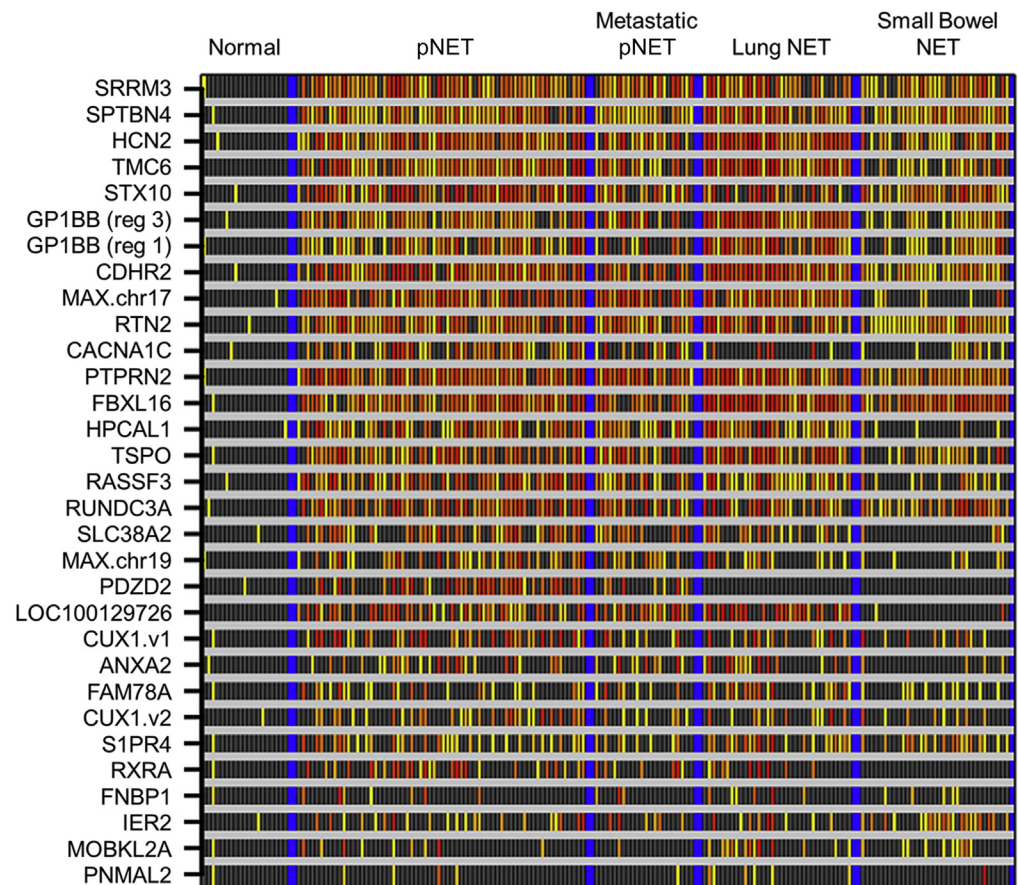


**Figure 2.** ACTB corrected methylation intensity in DNA markers assayed in normal tissue, primary pNETs, metastatic pNETs, and lung and small bowel NETs. Each column on the x-axis represents an individual patient’s sample; each row on the y-axis represents the methylation-specific PCR product by MSP assay for each marker.

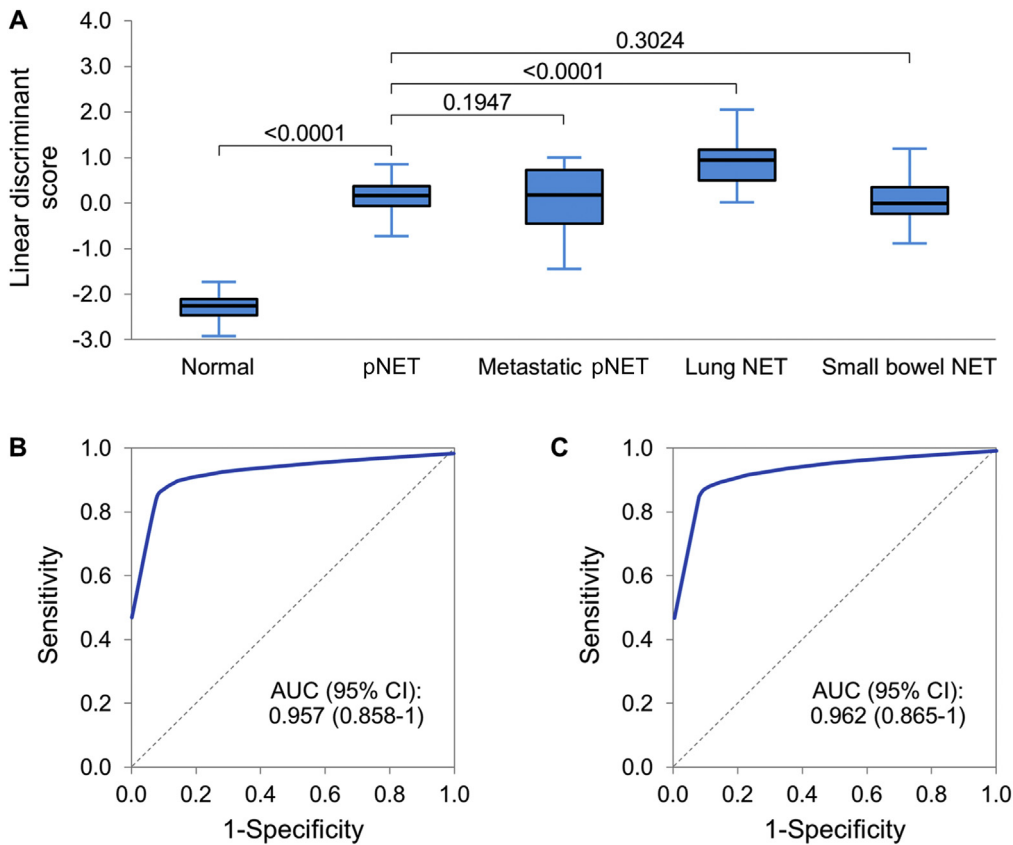


**Figure 3.** (A) Distribution of MDM panel linear discriminant score (LDS) comparing normal pancreas tissue to primary and metastatic pNET, primary lung NET, and small bowel NET. (B) Cross-validated ROC and AUC for primary pNET vs control. (C) Cross-validated ROC and AUC for metastatic pNET vs control.

metastatic pNET. Studies focusing on epigenetic alterations in pNETs are sparse, and the majority of published literature evaluate a limited set of candidate genes.<sup>10</sup> In a study focusing on genome-wide CpG methylation profiling of pNETs, Tirosh et al<sup>19</sup> studied 29 pancreatic tissue samples from nonfunctioning pNETs and concluded that aberrant methylation likely plays a key role in pNET initiation and/or progression, even in subjects with underlying driver mutations. In their study, the protein tyrosine phosphate receptor type N2 (*PTPRN2*) gene was noted to be significantly hypomethylated in von Hippel-Lindau syndrome, multiple endocrine neoplasia type 1, and sporadic pNETs. *PTPRN2* was one of the several MDMs identified in our study and demonstrated reasonable accuracy (AUC 0.91) for distinguishing pNET from normal pancreas tissue. *SRRM3*, another marker we identified, has neuronal splicing activity and is associated with the RE1-silencing transcription factor REST, which is a repressor in NETs.<sup>20</sup> The majority of the other MDMs identified in our study have known protein functions and oncogenic associations (Table A2). Identifying molecular similarities and differences between primary and metastatic tumor deposits from the same cancer not only enhances understanding of the biology of tumor progression but also is uniquely informative to the development of a diagnostic biomarker. Previous studies focusing on colon cancer have shown similar levels of candidate MDMs in DNA extracted from primary tumors and metastatic sites.<sup>21</sup> Our study is the first to compare DNA methylomes of paired

primary pNETs and pNET metastases as well as other primary pNETs in nonpancreatic tissue and yields similar conclusions. Although there is a growing body of evidence supporting the use of liquid biopsy approaches for diagnosis and monitoring treatment response in several different cancers, the only blood-based diagnostic molecular biomarker currently available for NETs is an mRNA-based biomarker, the NETest (Wren Laboratories, Branford, CT). In a recently published meta-analysis, this blood-based test was demonstrated to have high diagnostic accuracy, supporting clinical utility for both diagnosis and therapy monitoring.<sup>22</sup> The NETest (Wren Laboratories, Branford, CT) has also been shown to have a significantly higher diagnostic accuracy for gastroenteropancreatic and bronchopulmonary NETs than chromogranin A.<sup>23</sup> These findings indicate that exploring other molecular biomarker classes for plasma applications in diagnosis of pNETs may be informative. In previous studies, our group has demonstrated that plasma MDMs have high accuracy in detecting liver, colon, esophageal, gastric, and pancreatic cancer. MDMs with a high-plasma WBC background signal in non-diseased patients are not suitable for plasma-based assays. Our filtering criteria for tissue MDM discovery intentionally included markers that demonstrated only moderate accuracy in tissue but had near-perfect discrimination when comparing pNET tissue to normal buffy coat. This provides scientific rationale for future studies aimed at exploring these candidate MDMs in a blood-based application for

diagnosis of pNETs. Our study is not without limitations. First, we did not include other primary nonpancreatic NETs in our initial discovery phase that would have allowed identification of MDMs that discriminate between the different primary sites and provide information about the site of origin. However, we included a large subset of other primary sites in our validation stage and demonstrate the overlap in tissue methylation across sites. Second, we were limited in the total number of normal pancreas tissue samples for discovery, and this was necessitated by our stringent inclusion criteria of avoiding normal tissue from the resection margin of pNETs and a limited number of indications for resection of benign pancreatic disease. However, all tissue blocks used for this study were independently reviewed by an expert pancreas pathologist to confirm case and control allocation prior to DNA extraction to optimize accuracy and validity of study results. Finally, we did not have sufficient power to study the performance of tissue MDMs in specific syndromes associated with NETs such as von Hippel-Lindau syndrome or multiple endocrine neoplasia. There is a critical need for an accurate blood-based biomarker with applications in both diagnosis and surveillance of patients with pNETs. Based on the results of this tissue study and concomitant assessment of tissue and buffy coat methylation, we are uniquely poised for further development of MDMs as a circulating biomarker in pNETs.

## Supplementary Materials

Material associated with this article can be found in the online version at <https://doi.org/10.1016/j.gastha.2022.01.006>.

## References

1. Dasari A, Shen C, Halperin D, et al. Trends in the incidence, prevalence, and survival outcomes in patients with neuroendocrine tumors in the United States. *JAMA Oncol* 2017;3:1335–1342.
2. Hallet J, Law CH, Cukier M, et al. Exploring the rising incidence of neuroendocrine tumors: a population-based analysis of epidemiology, metastatic presentation, and outcomes. *Cancer* 2015;121:589–597.
3. Halfdanarson TR, Strosberg JR, Tang L, et al. The North American Neuroendocrine Tumor Society consensus guidelines for surveillance and medical management of pancreatic neuroendocrine tumors. *Pancreas* 2020;49:863–881.
4. Singh S, Chan DL, Moody L, et al. Recurrence in resected gastroenteropancreatic neuroendocrine tumors. *JAMA Oncol* 2018;4:583–585.
5. Singh S, Moody L, Chan DL, et al. Follow-up recommendations for completely resected gastroenteropancreatic neuroendocrine tumors. *JAMA Oncol* 2018;4:1597–1604.
6. Kisiel JB, Raimondo M, Taylor WR, et al. New DNA methylation markers for pancreatic cancer: discovery, tissue validation, and pilot testing in pancreatic juice. *Clin Cancer Res* 2015;21:4473–4481.
7. Majumder S, Raimondo M, Taylor WR, et al. Methylated DNA in pancreatic juice distinguishes patients with pancreatic cancer from controls. *Clin Gastroenterol Hepatol* 2019;18:676–683.e3.
8. Majumder S, Taylor WR, Yab TC, et al. Novel methylated DNA markers discriminate advanced neoplasia in pancreatic cysts: marker discovery, tissue validation, and cyst fluid testing. *Am J Gastroenterol* 2019;114:1539–1549.
9. Lakis V, Lawlor RT, Newell F, et al. DNA methylation patterns identify subgroups of pancreatic neuroendocrine tumors with clinical association. *Commun Biol* 2021;4:155.
10. Mafficini A, Scarpa A. Genetics and epigenetics of gastroenteropancreatic neuroendocrine neoplasms. *Endocr Rev* 2019;40:506–536.
11. Sun Z, Baheti S, Middha S, et al. SAAP-RRBS: streamlined analysis and annotation pipeline for reduced representation bisulfite sequencing. *Bioinformatics* 2012;28:2180–2181.
12. Li LC, Dahiya R. MethPrimer: designing primers for methylation PCRs. *Bioinformatics* 2002;18:1427–1431.
13. DeLong ER, DeLong DM, Clarke-Pearson DL. Comparing the areas under two or more correlated receiver operating characteristic curves: a nonparametric approach. *Biometrics* 1988;44:837–845.
14. Fisher RA. The use of multiple measurements in taxonomic problems. *Ann Eugen* 1936;7:179–188.
15. Kisiel JB, Dukek BA, Kanipakam RVSR, et al. Hepatocellular carcinoma detection by plasma methylated DNA: discovery, phase I pilot, and phase II clinical validation. *Hepatology* 2019;69:1180–1192.
16. Lennon AM, Buchanan AH, Kinde I, et al. Feasibility of blood testing combined with PET-CT to screen for cancer and guide intervention. *Science* 2020;369:eabb9601.
17. Liu MC, Oxnard GR, Klein EA, et al. Sensitive and specific multi-cancer detection and localization using methylation signatures in cell-free DNA. *Ann Oncol* 2020;31:745–759.
18. Majumder S, Taylor WR, Foote PH, et al. High detection rates of pancreatic cancer across stages by plasma assay of novel methylated DNA markers and CA19-9. *Clin Cancer Res* 2021;27:2523–2532.
19. Tirosh A, Mukherjee S, Lack J, et al. Distinct genome-wide methylation patterns in sporadic and hereditary nonfunctioning pancreatic neuroendocrine tumors. *Cancer* 2019;125:1247–1257.
20. Nakano Y, Wiechert S, Bánfi B. Overlapping activities of two neuronal splicing factors switch the GABA effect from excitatory to inhibitory by regulating REST. *Cell Rep* 2019;27:860–871.e8.
21. Orjuela S, Menigatti M, Schraml P, et al. The DNA hypermethylation phenotype of colorectal cancer liver metastases resembles that of the primary colorectal cancers. *BMC Cancer* 2020;20:290.
22. Öberg K, Califano A, Strosberg JR, et al. A meta-analysis of the accuracy of a neuroendocrine tumor mRNA genomic biomarker (NETest) in blood. *Ann Oncol* 2020;31:202–212.
23. Malczewska A, Witkowska M, Wójcik-Giertuga M, et al. Prospective evaluation of the NETest as a liquid biopsy for gastroenteropancreatic and bronchopulmonary

neuroendocrine tumors: an ENETS Center of excellence experience. *Neuroendocrinology* 2021;111:304–319.

Received September 28, 2021. Accepted January 25, 2022.

#### Correspondence:

Address correspondence to: Shounak Majumder, MD, Mayo Clinic, 200 First SW, Rochester, MN 55905. e-mail: [majumder.shounak@mayo.edu](mailto:majumder.shounak@mayo.edu).

#### Acknowledgments:

The authors are grateful for the Genome Analysis Core (GAC) and co-directors Julie M. Cunningham, Ph.D., and Eric Wieben, Ph.D. GAC is supported, in part, by the Center for Individualized Medicine and the Mayo Clinic Comprehensive Cancer Center grant (National Cancer Institute P30CA15083).

#### Authors' Contributions:

Shounak Majumder: Study concept and design; acquisition of data; analysis and interpretation of data; drafting of the manuscript; critical review of the manuscript for important intellectual content; obtained funding; study supervision. Thorvardur Halfdanarson: Study concept and design; interpretation of data; drafting of the manuscript; critical review of the manuscript for important intellectual content. Calise Berger: Laboratory testing and interpretation of data. Patrick Foote: Laboratory testing and interpretation of data. Xiaoming Cao: Laboratory testing and interpretation of data. Maria McGlinch: Laboratory testing and interpretation of data. Brianna Gysbers: Laboratory testing and interpretation of data. Jaime de La Fuente: Acquisition of data. Mariah Robran: Clinical research coordination. Karen Doering: Clinical research coordination and research program management. Kelli Burger: Study concept and design; study database management; formal statistical analysis; critical review of the manuscript for important intellectual content. William Bamlet: Identification of case and control tissue; Critical review of the manuscript for important intellectual content. Ann Oberg: Critical review of the manuscript for important intellectual content. Douglas Mahoney: Study concept and design; formal statistical analysis; critical review of the manuscript for important intellectual content. Rondell Graham: Study concept and design; study pathologist; critical review of manuscript for important intellectual content. William Taylor: Study concept and design; laboratory experimental design; analysis and

interpretation of data; critical review of the manuscript for important intellectual content. Gloria Petersen: Study concept and design; shared archival biospecimens for study; critical review of manuscript for important intellectual content. John Kisiel: Study concept and design; analysis and interpretation of data; critical review of the manuscript for important intellectual content; obtained funding; study supervision.

#### Conflicts of Interest:

Mayo Clinic and Exact Sciences have an intellectual property development agreement. These authors disclose the following: Drs Majumder, & Kisiel and Messrs. Taylor and Mahoney are listed as inventors under this agreement and could share potential future royalties as employees of Mayo Clinic. The remaining authors disclose no conflicts.

#### Funding:

Research reported in this publication was supported by the National Institute of Diabetes and Digestive and Kidney Diseases of the National Institutes of Health under the award number P30DK084567 (Mayo Clinic Center for Cell Signaling in Gastroenterology Pilot and Feasibility Award) to Dr Majumder. This work was partially supported by R37 CA214679 to Dr Kisiel and by P50 CA 102701 and U01 CA210138 to Dr Petersen. Drs Majumder and Petersen were also supported by a philanthropic gift to the Mayo Clinic for Early Detection of Pancreatic Cancer from the Centene Charitable Foundation. The content of this manuscript is solely the responsibility of the authors and does not necessarily represent the official views of the National Cancer Institute or the National Institutes of Health.

#### Ethical Statement:

The corresponding author, on behalf of all authors, jointly and severally, certifies that their institution has approved the protocol for any investigation involving humans or animals and that all experimentation was conducted in conformity with ethical and humane principles of research.

#### Data Transparency Statement:

Availability of data from a secure Mayo Clinic server is subject to approval from the authors, the Mayo Clinic Internal Review Board, and Exact Sciences. Availability of human bio specimen study materials is subject to approval from the Mayo Clinic Pancreatic Cancer SPORE Scientific Committee, the Mayo Clinic Internal Review Board, and Mayo Clinic. Analytic methods are included in the main manuscript.